Modeling and Analysis of a Membrane-Based Randomized-Contact Decoder

Jennifer Long and John E. Savage

Computer Science, Brown University
Providence, RI 02912-1910, jes@cs.brown.edu

ABSTRACT

Decoders are employed to address individual NWs in crossbars (xbars) used for storage and computation. We report on the simulation and analysis of a membrane-based nanowire (NW) decoder proposed by Pribat and Savage [1] that implements the randomized-contact decoder (RCD) introduced by Williams and Kuekes [2] and analyzed by Hogg *et al* [3] and Rachlin and Savage [4]. An RCD has two sets of parallel wires, NWs and mesoscale wires (MWs), that are orthogonal to one another. "Contacts" are made at random at NW/MW junctions. These contacts, which allow a MW to control a NW, assign codewords to NWs, some of which are unusable. In the membrane-based decoder a contact is made by filling a pore with a metallic pin. As the probability of filling pores increases, the probability of creating a MW/NW contact increases monotonically. However, the average number of usable NW addresses achieves a maximum when a small fraction of the pores is filled. The goal is to maximize the average number of usuable NW addresses. We report on the results of our simulations of the membrane-based RCD as well as corroborate the experimental results with analysis of probabilistic models.

Keywords: crossbars, memories, decoders, nanowires

1 Introduction

Nanowire (NW) xbars (see Figure 1) provide a promising basis for nanoscale devices such as electronic memory and logic circuits [5]–[8]. To form an xbar, two groups of parallel nanowires are placed orthogonally with programmable molecules (PMs) between them. The PMs at NW crosspoints are switched between open and a diode by applying a positive or negative electric field. NW xbars can be used as storage units or programmed logic arrays. Storage densities as high as 10^{11} bits/cm^2 have been achieved [9].

To achieve high storage densities a method for controlling NWs with mesoscale wires (MWs) must be used. Given that MWs are an order of magnitude larger than NWs, it does not suffice to attach one MWs to each NW. Three basic techniques have been proposed to control NWs with MWs. The first (FET-based) assumes that segments of each NW can be "opened" by electric fields applied by MWs. (They act like field effect transistors.) [5], [6], [10]–[12]. The second (CMOL) assumes that nanoscale pins are grown at crosspoints of a MW xbar that make contact with NWs in a NW xbar by passing through the openings between NWs [13]. The third places two electrodes on either side of a small set of lightly-doped NWs and applies a graduated electric field that depletes the carriers in all but one NW [14].

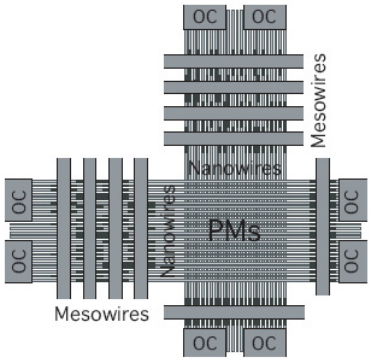

Figure 1: A NW xbar with programmable molecules (PMs) at NW crosspoints. A small number of NWs is connected between ohmic contacts (OCs). A NW is addressed by selecting and OC pair and deactivating all but one NW by applying fields to MWs. Data is stored at a crosspoint by applying a large electric field across it. Data is sensed with a smaller field.

All three techniques introduce randomness in the connections between NWs and MWs. This is unavoidable when the NW pitch is 15-20 nms or less; here lithography is either too coarse or too expensive. Each technique assigns addresses to NWs that are not predictable in advance. A separate memory is needed to map from contiguous external addresses to internal ones.

Three general methods of realizing FET-based decoders have been proposed. The **encoded nanowire decoder**, assumes that NWs are lightly-doped in some sections along their length and heavily-doped elsewhere and assembled fluidically [10], [15]. Lightly-doped regions are placed in NWs during growth [16]–[18] or exposed by etching NWs that are radially encoded with differentially etcheable shells [12]. The latter method

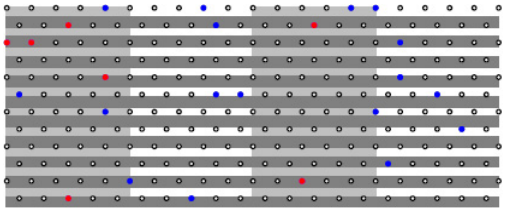

Figure 2: The membrane-based RCD has metal-filled pores placed at random between MWs (light grey) and NWs (dark grey). The red (blue) dots denote filled pores whose centers overlap (don't overlap) a NW.

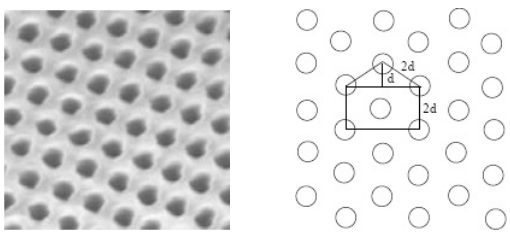

Figure 3: Regular pores in aluminum oxide and a model hexagonal lattice.

avoids misalignment arising in the former. The **mask-based decoder**, assumes that a regular array of uniform NWs [19], [20] is first placed on a chip. High-K dielectric rectangles are deposited between some NWs and MWs [11]. A NW is controllable by a MW if there is rectangle between them. The **randomized-contact decoder (RCD)** (see Figure 2) also assumes uniform NWs. It assumes that a "contact" (equivalent to a FET) is made at random between NWs and MWs.

We report on simulation and analysis of the membrane-based RCD. Membranes can be created by anodizing a thin aluminum film deposited between NWs and MWs to form hexagonal pores. (See Figure 2.) When pores are filled at random with metal or a high-K dielectric, an electric field applied to MWs creates a FET in lightly doped NWs. We investigate the number of usuable NWs resulting from random assembly as a function of the sizes of NWs and MWs and the fraction of filled pores. We believe that RCDs are among the most promising methods of controlling NWs in xbars.

2 The Membrane-Based Decoder

It is assumed that pores form a hexagonal lattice, as shown in Figure 3. The pore lattice is created and rotated to a preset angle relative to the MWs and pores filled at random.

Let λ_{meso}, λ_{nano} be the width and separation of MWs and NWs. (Their pitch is twice their width.) Let $2d_{pore}$ be the center to center pore spacing in the pore lattice (see Figure 3) and let θ be the rotation angle of

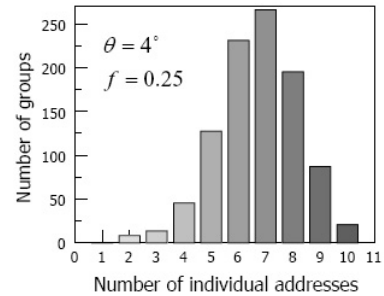

Figure 4: A histogram of N_a, the number of i.a. NWs in 1000 groups of 10 NWs. The rotation angle is 4 degrees and the fraction of pores filled is 0.25.

the pore lattice relative to NWs. Finally, let f be the fraction of filled pores in the lattice and n be the number of runs of the program.

The simulator chooses pores to fill by picking two random integers u and v treated as row and column indices. These integers are mapped to physical positions based on the dimensions of the lattice, its displacement, and the angle between NWs and MWs. Pores are filled until a preset fraction f of the pores are filled.

A pore forms a NW/MW contact if the pore center overlaps both (red dots in Figure 2). A MW **controls** a NW if there is at least one filled pore between them. Let there be N NWs and M MWs. Let ν_i by the ith NW, $1 \leq i \leq N$, and let μ_j be the jth MW, $1 \leq j \leq M$. ν_i has **codeword** $\mathbf{c}_i$ in which the jth component, $c_{i,j}$, is 1 if μ_j controls ν_i and 0 otherwise. If $c_{i,j} = 1$ and an electric field is applied to μ_j, ν_i is turned off.

Codeword $\mathbf{c}_r$ **implies** the codeword $\mathbf{c}_s$ ($\mathbf{c}_r \Rightarrow \mathbf{c}_s$) if for each $1 \leq j \leq M$ $c_{r,j} \Rightarrow c_{s,j}$ where the latter holds if and only if $c_{s,j}$ is 1 whenever $c_{r,j}$ is 1. Otherwise, it is unconstrained. Clearly, $010 \Rightarrow 110$.

If $\mathbf{c}_r \Rightarrow \mathbf{c}_s$, whenever fields are applied to MWs that leave $\mathbf{c}_r$ on, $\mathbf{c}_s$ is also on. Thus, the two NWs cannot be controlled independently. We say that the ith NW with codeword $\mathbf{c}_i$ is **individually addressable (i.a.)** if for no other codeword $\mathbf{c}_s$ does $\mathbf{c}_s \Rightarrow \mathbf{c}_i$. Consider the codewords 010 and 110. The NW with codeword 110 is on when no field is applied to the first two MWs. But in this case, the other NW is also on. To determine if $\mathbf{c}_r \Rightarrow \mathbf{c}_s$, associate with each codeword its set of "1" positions and then test for containment of these sets.

The simulator is given N and M as well as $\rho = \lambda_{meso}/\lambda_{nano}$, $r = \lambda_{nano}/d$ (d is the pore diameter), θ, and f, the fraction of filled pores. It was run 1000 times to produce 1000 sets of N NW codewords. The simulator reports the number of controllable NWs as well as N_a, the number of i.a. NWs. A histogram of N_a is shown in Figure 4 when $\theta = 4°$ and $f = 0.25$. In 992 of 1000 address groups all NWs were controllable. N_a for these controllable groups is 6.71.

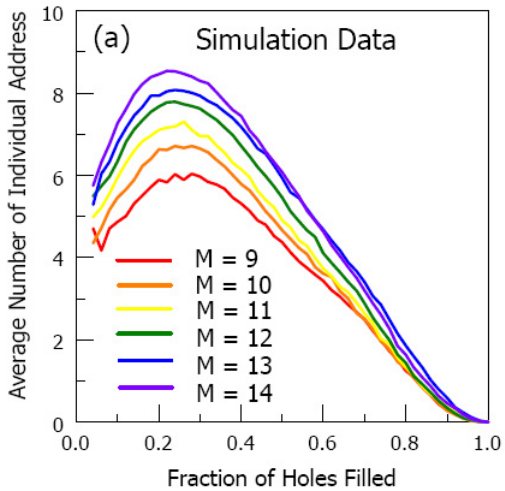

Figure 5: N_a as a function of f, the fraction of pores filled when $N = 10$, $r = 1$, $\theta = 15°$, and $\rho = 1$.

3 Simulation Results and Analysis

The simulator was used first to study the impact of θ and f. θ is important because when $r = 1$ and θ is a multiple of 60°, the number of controllable NWs is zero.

To study the effect of θ, we ran 1,000 simulations with $N = M = \rho = 10$, $r = 1$, and $f = 0.25$ at $\theta = 1°, 61°$ and multiples of 6°. We found that N_c, the average number of controllable NWs, was almost exactly N and N_a was between about 6.8 and 7.0. We conclude that the rotation angle is unimportant in the simulation except if close to a multiple of 60°. Because in practice pores do not form a perfect hexagonal pattern, the rotation angle should not be important.

We studied the effect of the fraction f of filled pores on N_c, and N_a by setting $\theta = 15°$. N_c grows monotonically with f and has a sharp transition from 0 to 1 as f increases from 0.05 to 0.2 or less, depending on the value of M. This phase transition has been seen before [3]. The more pores that are filled, the higher is the probability that a NW can be controlled by a MW.

Figure 5 shows that N_a is increases with M and has a single maximum at about $f = 0.25$. Experiments show the maximum increasing with pore diameter. N_a increases with M because NW codewords are more likely to be i.a. when M is large. The maximum in f reflects the fact that codewords are more likely to be similar (imply one another) when f is small or large.

We now explain the simulation results through probabilistic analysis. Let $a_{i,j}$ denote the number of pores at the ν_i/μ_j junction. Then, $A_i = \sum_{j=1}^{M} a_{i,j}$ is the total number of pores in all junctions between ν_i and MWs. Let $p_{i,j}$ ($q_{i,j} = 1 - p_{i,j}$) be the probability that ν_i is (is not) controlled by μ_j. A NW is controlled if one or more pores between and a MW are filled. It follows that

$$p_{i,j} = 1 - q_{i,j} = 1 - (1 - f)^{a_{i,j}}$$

Let P_i ($Q_i = 1 - P_i$) be the probability of that ν_i is (is not) controlled. It follows $Q_i = \prod_{j=1}^{M} q_{i,j} = (1 - f)^{A_i}$ and $P_i = 1 - Q_i = 1 - (1 - f)^{A_i}$. A group of NWs is controllable when each NW in the group is controllable. Since pores are filled independently, each NW is independent and the probability P' that all N NWs are controllable satisfies

$$P' = \prod_{i=1}^{M} P_i = \prod_{i=1}^{M} \left[1 - (1 - f)^{A_i}\right]$$

Applying the inequality between arithmetic and geometric means, twice and simplifying we have the following.

$$P' \leq \left(1 - (1 - f)^{M\bar{a}}\right)^N$$

Here $\bar{a} = (\sum_{i=1}^{N} A_i)/(MN)$ is the the average number of pores per junction.

Computing P' when $f \approx 0.20$, $N = 10$, $M = 10$ and $\theta = 15°$ and $\bar{a} = 3.0$ (obtained from simulations) shows that $P' \leq (1 - (1 - 0.20)^{30})^{10} = 0.987$ which is slightly larger than the simulation result, 0.975.

Consider next N_a. NW ν_i has codeword $\mathbf{c}_i$. ν_i is i.a. if there is no ν_s such that $\mathbf{c}_s \Rightarrow \mathbf{c}_i$. The probability that that NW ν_i is not i.a. is the probability that for some $s \neq i$, $c_s \Rightarrow c_i$. From the union bound, $P(\nu_i \text{ is not i.a.}) \leq \sum_{s \neq i} P(c_s \Rightarrow c_i)$.

$$P(\nu_i \text{ is i.a.}) \geq 1 - \sum_{s \neq i} P(c_s \Rightarrow c_i)$$

But $c_s \Rightarrow c_i$ if and only if $c_{s,k} \Rightarrow c_{i,k}$ for all $1 \leq k \leq M$ which holds when $c_{s,k} = 1$ and $c_{i,k} = 0$ does not occur. Thus, $P(c_{s,k} \Rightarrow c_{i,k}) = p_{s,k} q_{i,k}$. Recall that $p_{i,j} = 1 - (1 - f)^{a_{i,j}}$. $a_{s,k}$ and $a_{i,k}$ may be statistically dependent. However, $p_{s,k}$ and $p_{i,k}$ are statistically independent when $a_{s,k}$ and $a_{i,k}$ are fixed. Thus,

$$P(c_{s,k} \Rightarrow c_{i,k} | a_{s,k} a_{i,k}) = 1 - (1 - (1 - f)^{a_{s,k}})(1 - f)^{a_{i,k}}$$

To procede we assume that $a_{s,k}$ and $a_{i,k}$ are statistically independent, an assumption tested below. Averaging all choices for $a_{s,k}$ and $a_{i,k}$, we have

$$P(\nu_i \text{ is i.a.}) \geq 1 - (N - 1)(1 - pq)^M$$

where $q = \sum_{a_{r,k}} (1 - f)^{a_{r,k}} P(a_{r,k})$. It follows that $N_a \geq N \cdot [1 - (N - 1) \cdot (1 - pq)]^M$.

We measured $P(a_{i,j})$ when $N = 10$, $M = 10$, $\rho = 1$, $r = 1$ and $\theta = 15°$. In this case $0 \leq a_{i,j} \leq 6$. We found

x	0	1	2	3	4	5	6
$P(x)$	0.0	0.02	0.38	0.34	0.13	0.07	0.06

The theoretical and simulation results both give maximums in N_a when $f \approx 0.24$. When $f = 0.24$, $q \approx 0.457$ and $p = 1-q \approx 0.543$, and the analytical lower bound to $N_a \approx 4.81$, which is somewhat less than the simulation result of 6.75 but comparable given the estimates that have been made.

4 Conclusions

The membrane-based randomized contact decoder provides a promising implementation of a NW decoder. It obviates the technical difficulty of precisely positioning contacts on the nano-scale. It can also cope with fabrication defects present in the nano-scale xbar. The simulations and analysis presented here advance our understanding of the potential of this technology by showing that the number of individually addressable NWs is largest for a number of MWs between 9 and 14 when the fraction of filled pores $f \approx .25$, a resulted supported by analysis.

Work supported in part by NSF Grant CCF-0403674.

REFERENCES

[1] Didier Pribat and John E. Savage. Membrane-based randomized-contact decoders. Technical report, Computer Science Department, Brown University, February 26 2007.

[2] R. S. Williams and P. J. Kuekes. Demultiplexer for a molecular wire crossbar network, US Patent Number 6,256,767, July 3, 2001.

[3] Tad Hogg, Yong Chen, and Philip J. Kuekes. Assembling nanoscale circuits with randomized connections. *IEEE Trans. Nanotechnology*, 5(2):110–122, 2006.

[4] Eric Rachlin and John E Savage. Nanowire addressing with randomized-contact decoders. In *Procs. ICCAD*, pages 735–742, November, 2006.

[5] P. J. Kuekes, R. S. Williams, and J. R. Heath. Molecular wire crossbar memory, US Patent Number 6,128,214, Oct. 3, 2000.

[6] André DeHon. Array-based architecture for FET-based, nanoscale electronics. *IEEE Transactions on Nanotechnology*, 2(1):23–32, Mar. 2003.

[7] André DeHon, Seth Copen Goldstein, Philip Kuekes, and Patrick Lincoln. Nonphotolithographic nanoscale memory density prospects. *IEEE Transactions on Nanotechnology*, 4(2):215–228, 2005.

[8] André DeHon. Nanowire-based programmable architectures. *J. Emerg. Technol. Comput. Syst.*, 1(2):109–162, 2005.

[9] Jonathan E. Green, Jang Wook Choi, Akram Boukai, Yuri Bunimovich, Ezekiel Johnston-Halperin, Erica DeIonno, Yi Luo, Bonnie A. Sheriff, Ke Xu, Young Shik Shin, Hsian-Rong Tseng, J. Fraser Stoddart, and James R. Heath. A 160-kilobit molecular electronic memory patterned at 1011 bits per square centimetre. *Nature*, 445:414–417, 2006.

[10] André DeHon, Patrick Lincoln, and John E. Savage. Stochastic assembly of sublithographic nanoscale interfaces. *IEEE Transactions on Nanotechnology*, 2(3):165–174, 2003.

[11] Robert Beckman, Ezekiel Johnston-Halperin, Yi Luo, Jonathan E. Green, and James R. Heath. Bridging dimensions: Demultiplexing ultrahigh-density nanowire circuits. *Science*, 310:465–468, 2005.

[12] John E. Savage, Eric Rachlin, André DeHon, Charles M. Lieber, and Yue Wu. Radial addressing of nanowires. *J. Emerg. Technol. Comput. Syst.*, 2(2):129–154, 2006.

[13] K. K. Likharev and D. B. Strukov. Cmol: Devices, circuits, and architectures. In G. Cuniberti *et al.*, editor, *Introduction to Molecular Electronics*, pages 447–477, 2005.

[14] K. Gopalakrishnan, R. S. Shenoy, C. Rettner, R. King, Y. Zhang, B. Kurdi, L. D. Bozano, J. J. Welser, M. B. Rothwell, M. Jurich, M. I. Sanchez, M. Hernandez, P. M. Rice, W. P. Risk, and H. K. Wickramasinghe. The micro to nano addressing block. In *Procs. IEEE Int. Electron Devices Mtng.*, Dec. 2005.

[15] Benjamin Gojman, Eric Rachlin, and John E Savage. Decoding of stochastically assembled nanoarrays. In *Procs 2004 Int. Symp. on VLSI*, Lafayette, LA, Feb. 19-20, 2004.

[16] Mark S. Gudiksen, Lincoln J. Lauhon, Jianfang Wang, David C. Smith, and Charles M. Lieber. Growth of nanowire superlattice structures for nanoscale photonics and electronics. *Nature*, 415:617–620, February 7, 2002.

[17] Yiying Wu, Rong Fan, and Peidong Yang. Block-by-block growth of single-crystal Si/SiGe superlattice nanowires. *Nano Letters*, 2(2):83–86, 2002.

[18] M. T. Björk, B. J. Ohlsson, T. Sass, A. I. Persson, C. Thelander, M. H. Magnusson, K. Deppert, L. R. Wallenberg, and L. Samuelson. One-dimensional steeplechase for electrons realized. *Nano Letters*, 2(2):87–89, 2002.

[19] G. Y. Jung, S. Ganapathiappan, A. A. Ohlberg, L. Olynick, Y. Chen, William M. Tong, and R. Stanley Williams. Fabrication of a 34x34 crossbar structure at 50 nm half-pitch by UV-based nanoimprint lithography. *Nano Letters*, 4(7):1225–1229, 2004.

[20] E. Johnston-Halperin, R. Beckman, Y. Luo, N. Melosh, J. Green, and J.R. Heath. Fabrication of conducting silicon nanowire arrays. *J. Applied Physics Letters*, 96(10):5921–5923, 2004.